ELSEVIER

Contents lists available at ScienceDirect

Quaternary Science Reviews

journal homepage: www.elsevier.com/locate/quascirev



The effects of external forcing agents on the biodiversity and species richness associated with the environmental history of Louisiana's wetlands over the late Holocene



Junghyung Ryu ^{a, *}, Kam-biu Liu ^a, Terrence A. McCloskey ^b

- ^a Department of Oceanography and Coastal Sciences, College of the Coast and Environment, Louisiana State University, Energy, Coast & Environment Building, Baton Rouge, LA, 70803, USA
- ^b St. Margarets Village, Mile 32 Hummingbird Highway, Belize, Central America, USA

ARTICLE INFO

Article history: Received 16 August 2022 Received in revised form 1 November 2022 Accepted 4 November 2022 Available online xxx

Handling Editor: Donatella Magri

Keywords:
Environmental change
Biodiversity
Global change
Multivariate principal component analysis
Coastal wetland sustainability
Mississippi delta
Palynology

ABSTRACT

This study evaluates plant diversity and species richness levels and reconstructs the environmental history of a site near Little Lake in southeast Louisiana, USA over the past 3200 years. Six successive ecosystems occurred as a result of changing environmental conditions, ranging from the local (anthropogenic activities), regional (delta lobe switching), and to global (sea level rise): interdistributary bay (3.2 –2.3 cal kyr BP), hydrophytic freshwater marsh (2.3–1.42 cal kyr BP), mesophyte coastal prairie (1.42 –0.92 cal kyr BP), *Typha* marsh (0.92–0.33 cal kyr BP), intermediate marsh (0.33 cal kyr BP – ad, 1972 CE), brackish marsh (197 CE2-present). Biodiversity was evaluated for each ecosystem, with maximum diversity occurring during the period of maximum delta-growth as the river dynamics increased landscape heterogeneity by creating diverse habitats, including marsh, swamps, oxbow lakes, and natural levees, while the transgressive phase presents the lowest biodiversity due to increasing salinity. Multi-variate analysis is used to identify the primary depositional processes for each stage and infer the proximate forcing agents(s). Early ecosystem shifts were controlled by the stages of the delta cycle, while more recent shifts are associated with anthropogenic activities and the effects of global climate change such as sea-level rise, and more intense tropical cyclones.

© 2022 Elsevier Ltd. All rights reserved.

1. Introduction

Globally, large river deltas are of great societal significance due to their economic importance as transport and industrial hubs (Authority, 2020). Due to rising sea level and associated effects of global warming many of these economically important deltas are facing severe stresses, including oceanic transgression, subsidence, and the deleterious effects of intense storms. On the world's vulnerable coasts low-lying river deltas in Asia, Europe, and USA., face immediate threats of sinking land (Schmidt, 2015), coastal flooding, and loss of infrastructure (Syvitski et al., 2009). Understanding the underlying agents driving these processes is, of course, the necessary first step in maintaining the viability of these deltas. The rapid coastal retreat affecting the Mississippi River Delta and its

Roughly 40% of the U.S.'s continental wetlands occur in coastal Louisiana, which contains a large and diverse set of ecosystems, ranging from saltwater marshes and mangrove forests through freshwater swamps (Couvillion et al., 2017). However, coastal erosion has been severe, with oceanic transgression resulting in the loss of ~5000 km² of land since 1930 (Couvillion et al., 2017). Typically, salinity and marine conditions progress landward, with saline marshes/mangrove forests becoming open water, brackish marshes transitioning to salt marshes, fresh marshes becoming

E-mail addresses: jhrainlv7@gmail.com (J. Ryu), kliu1@lsu.edu (K.-b. Liu), tamccloskey2014@gmail.com (T.A. McCloskey).

surrounding wetlands is a particularly important example as 18% of the United States' oil supply flows through Louisiana, amounting to \$44 billion annually, with 380,000 jobs tied to the cargo handled through the port of New Orleans (Authority, 2020). The coastal wetlands are the key element in sustaining both the social and commercial infrastructures, as they both attenuate power of intense storms, and provide the physical foundation of all activities. The single most important factor in determining the sustainability of these wetlands is the vegetative response of each individual ecosystem to the stresses they are currently facing.

^{*} Corresponding author.

brackish, and bottomland forests becoming fresh marshes. In an effort to achieve a sustainable coast, the state of Louisiana has designed and funded a vast number of projects, codified under the Coastal Master Plans (Authority, 2020), the overarching objective being to produce sustainable ecosystems capable of retaining soil, retard erosion during storm events, and accrete upward through the deposition of autochthonous material. Clearly, to obtain this goal it is necessary to understand and address local conditions. Recognizing the existence of temporal and spatial variability in the relative importance of the various external agents driving the processes controlling coastal migration is the essential first step in identifying the controls over the biological, chemical, and geological processes occurring at any specific site. This knowledge can then be applied to develop local strategies, which can be combined on the state and regional level in order to combat coastal retreat, and, potentially, be as models globally.

Due to the effects of the Mississippi River, the Louisiana coast is extremely dynamic, chemically, geologically, and geomorphologically. Throughout the late Holocene, in the process known as 'lobe switching', the distributaries of the Mississippi River have wandered across the state, making abrupt locational shifts as the existing channel becomes hydraulically (fluvially) inefficient. At any location, the existent ecosystem is highly dependent on the state/proximity of the concurrent delta lobe. In areas affected by a delta lobe freshwater ecosystems colonize the delta plain, while brackish and saline ecosystems occur at a distance (Ryu et al., 2021a). In unaffected areas vegetation dynamics are controlled by other factors.

The specifics of each vegetation community are determined by a large number of factors, including elevation, salinity, hydroperiod, and the amount of sediment and water delivered. All of these factors are highly variable over both time and space and affect vegetation composition, diversity, and richness.

Although palynology-based paleoenvironmental reconstruction is an effective method for elucidating long-term ecosystem dynamics, the assessment of the level of biodiversity and vegetative richness is not usually a part of such reconstructions. Plant diversity is controlled by multiple factors including climate, habitat heterogeneity, competition, and energy availability (Currie et al., 2004). Community composition and diversity levels can be extremely fluid along the Louisiana coast, as geomorphological, chemical, and hydrological background parameters can change rapidly due to such factors as sea-level rise (SLR), subsidence, storm surge, lobe switching, etc. (Ryu et al., 2021b). Although rarefaction analysis of biodiversity based on fossil pollen data has been used to estimate vegetation diversity and richness in England (Birks and Line, 1992), Colombia (Weng et al., 2006; Palazzesi et al., 2014), and Sweden (Berglund et al., 2008), this type of assessment has rarely been applied in the United States, Recent studies (Ryu et al., 2021b, 2022b) have used multivariate statistical techniques to reconstruct paleoenvironments for freshwater marsh and mangrove swamps in coastal Louisiana over the late Holocene, with an emphasis on identifying the underlying driver(s) of each ecosystem transition. In this study, we apply the same methodology to a currently brackish environment, namely a brackish marsh located near Little Lake in southeast Louisiana. Multivariable statistical analysis is conducted on geological, geochemical, and ecological data, and biodiversity and species richness are assessed for the last 3200 years. The overall goal is to identify the underlying agent(s) driving each transition. Identifying the dominant agent(s) forcing ecosystem/ diversity transition at specific times increases our understanding of ecosystem dynamics and provides clues regarding potential future ecosystem responses. This study breaks new ground as, to date, no studies have considered the effects of the relative importance of external forcing agents on biodiversity and species richness.

2. Study site

2.1. Geological setting

The study site (29°33′51.94″N, 90°12′33.00″W) is a brackish marsh located adjacent to the northern edge of Little Lake, in southeast Louisiana, ~45 km southwest of New Orleans (Fig. 1). Little Lake has an average depth of 1.5 m and is connected hydrologically to Lake Salvador in the north and to Barataria Bay in the south. Water sources for Little Lake are multiple; freshwater flows from the north through Bayou Perot and Bayou Rigolettes, from canals connected to Bayou Lafourche in the west, and the Mississippi River to the east, while saline water from the Gulf of Mexico enters through Barataria Bay (Fig. 1). Water level is variable as the site is subjected to seasonal floods.

Although historically from the early 1700s (Moore, 1899), the marshes surrounding Little Lake were fresh, they currently range from intermediate in the north to brackish in the south, with vegetation type dependent on salinity, elevation, and topography (Boesch, 1982). In general, salinity has increased over the last few decades as a result of severe land loss associated with relative sealevel rise (RSLR), driven by both natural and anthropogenic impacts, including SLR, subsidence, logging canals, and the constructions of dams and levees (Boesch, 1982).

Barataria Basin, ~110 km long and 50 km wide (Conner and Day, 1987), is located between the Mississippi River and the Bayou Lafourche distributaries. The basin began forming between 4000 and 3000 years ago as a result of the growth of St. Bernard and Lafourche delta lobes (Frazier, 1967). The basin assumed its current shape ~2000 years ago as St. Bernard and Lafourche subdeltas delivered freshwater and sediment to the Barataria Basin (Saucier, 1968).

Although salinity generally increases toward the south across the entire swath of the Louisiana wetlands, the gradient is not unidirectional with disjunct pockets of anomalous ecosystem types occurring as a result of local conditions. One example is the significant amount of freshwater marsh occurring along the southern end of the Baliz Delta (Fig. 1A). This spatial variability emphasizes the need for site-specific solutions.

2.2. Sea level and subsidence

Land subsidence rates, a result of the dewatering of fine-grain sediments, are highly variable along the coast of the Gulf of Mexico (Gonzalez and Törnqvist, 2009), meaning that relative sealevel rates are also highly variable spatially. Although eustatic sealevel rise (SLR) was rapid (~3.5 mm/yr) along the northern coast of the Gulf of Mexico before ~ 7000 BP, nearly 30 sea-level index points from the Mississippi River Delta show the SLR (~1.5 mm/yr) after 7000 BP, with no observable middle Holocene highstand (Tornqvist et al., 2004). Because coastal Louisiana consists almost entirely of fine-grain sediments delivered by the Mississippi River, subsidence is significant, but highly variable spatially, as the underlying sediments compact due to dewatering (Törnqvist et al., 2008). The subsidence, coupled with eustatic SLR, results in current RSLR rates for coastal Louisiana between 5 and 12 mm/yr (Jankowski et al., 2017). Over the last few decades, subsidence and erosion have enlarged lakes and converted marshes into interconnected water bodies (Conner and Day, 1987).

2.3. Ecological setting

The study site is a brackish marsh although salinity is seasonally variable, ranging from 0.2 ppt (July 2019) to 21.9 ppt (October 2019) (Authority, 2020). Organic sedimentary matter is autochthonous,

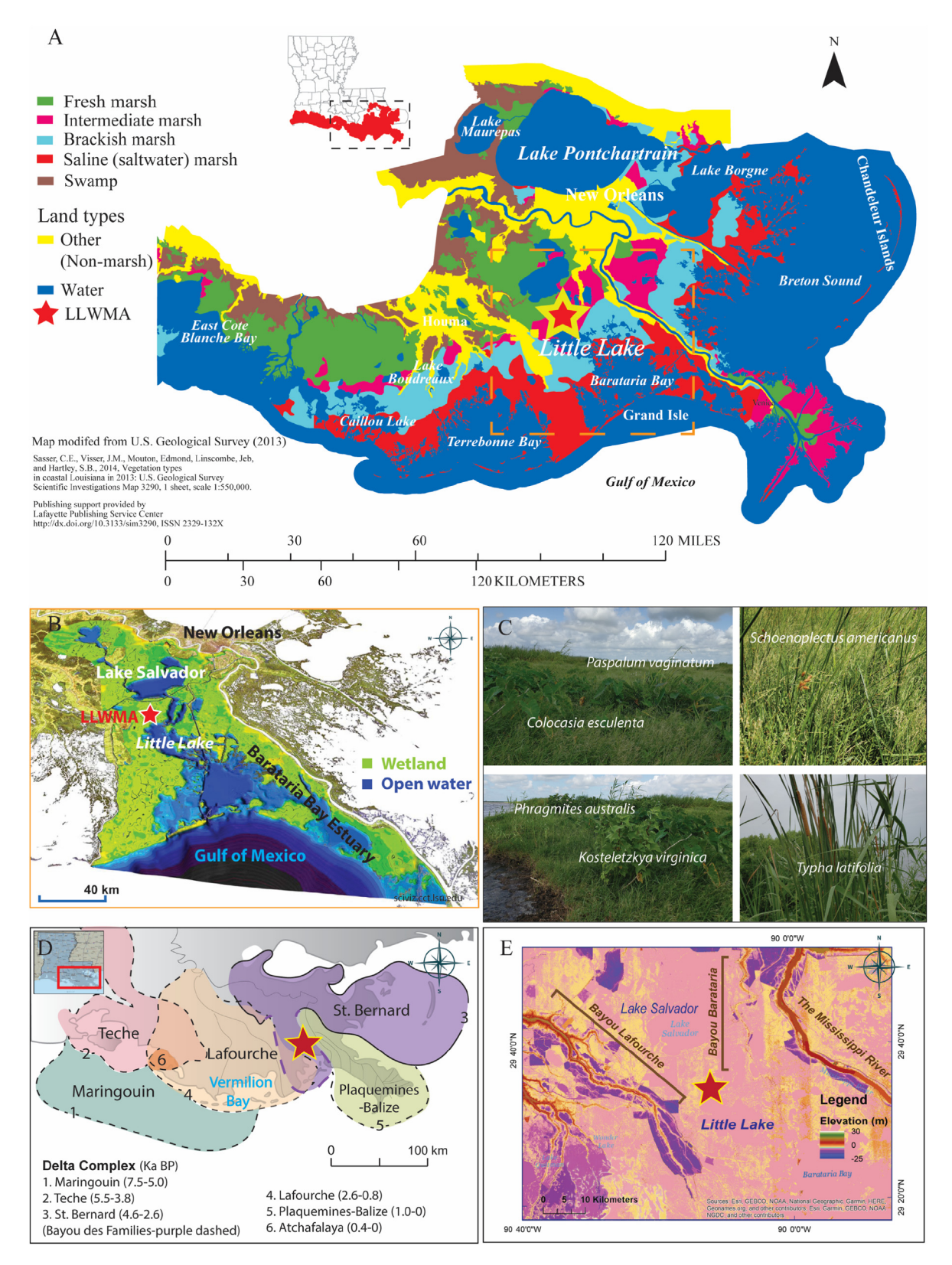


Fig. 1. Map of study site. (A) Vegetation types across the coastal wetlands in Louisiana. The orange box indicates Barataria Basin. (B) A DEM map of Barataria Basin depicting the Barataria Bay Estuary and study site (LLWMA). (C) Vegetation community at the study site. (D) Schematic representation of the Mississippi Delta complex; Spatial extent and age ranges of delta lobes in relation to study site (a star). (E) Digital elevation map shows the proximity of the Bayou Barataria and Bayou Lafourche. Maps were produced using ArcGIS 10.3 (A, B, E) and the ecosystem data from U.S Geological Survey, 1997 (sciviz.cct.lsu.edu). (For interpretation of the references to color in this figure legend, the reader is referred to the Web version of this article.)

derived from the marsh vegetation, while the mineral material is allochthonous, delivered either fluvially or by storm surges (Boesch, 1982). The local vegetation mainly consists of grass (paspalum vaginatum), common reed (Phragmites australis), bulrush (Schoenoplectus americanus), rosemallow (Hibiscus laevis), cowpea (Vigna luteola), cattail (Typha), arrowhead (Sagittaria), southern amaranth (Amaranthus australis), groundseltree (Baccharis halimifolia), and seashore mallow (Kosteletzkya virginica). Plant composition is highly affected by salinity and water level (Authority, 2020).

2.4. Anthropogenic setting

Although native Americans were living in the area since at least 1900 years BP, the major human disturbance began with the French and Spanish use of the surrounding area for agriculture, logging, and other economic and residential purposes from 1722 to 1779, resulting in significant swamp-to-marsh transitions (Yakubik et al., 1996). Bayou Lafourche was dammed in 1904, reducing freshwater input (Frazier, 1967). Other activities include the dredging of canals and, recently, freshwater diversions (Day et al., 2016; Xu et al., 2019), which have increased freshwater input to the basin.

3. Materials and methods

In June 2018, sediment cores were retrieved using a vibracorer from a brackish marsh adjacent to Little Lake (29°33′51.94″N, 90°12′33.00″W), in an area of aquatic and wetland vascular plants such as *Paspalum vaginatum*, *Sagittaria*, and *Typha* (Fig. 1C). The collected cores 90 cm (LLWMA1), 130 cm (LLWMA2), and 487 cm (LLWMA3), were transported to the LSU Global Paleoecology Lab in the Department of Oceanography and Coastal Sciences at Louisiana State University, where they were cut into 1–2 m sections and stored in a refrigerated room (4 °C) for further analyses.

3.1. Sedimentary analyses

The cores (LLWMA1, LLWMA2, LLWMA3) were split longitudinally and photographed after which visual and macrofossil analyses were conducted. The Munsell color chart was used for identifying sediment colors (Malacara, 2003) and conventional macrofossil analysis (Shirazi et al., 1988) was employed in constructing sedimentary fossil profiles (shell and plant debris). Loss-on-ignition (LOI), measuring water, organic, carbonate contents, and residuals (mainly silicates) was performed at a 1-cm interval on LLWMA3, following the conventional methodology (Dean, 1974). Based on the LOI results, grain-size was measured at 5–20 cm intervals, by wetsieving particles <2000 μm and dry-sieving particles >2000 μm . GRADISTAT (Blott and Pye, 2001) was used to calculate mean grain size, sorting, skewness, and kurtosis, with sample type and textural group reported for each sample (Table S5).

3.2. Geochronology

Core chronology was developed using accelerator mass spectrometry (AMS) and radiochemical analyses of 210 Pb (natural 238 U series, $t_{1/2}=22.2$ years) and 137 Cs (thermonuclear byproduct fallout, $t_{1/2}=30.1$ years). Organic materials (plant debris) from 92, 173, 230, and 292 cm, and an intact shell from 464 cm were extracted from LLWMA3 and sent to International Chemical Analysis, INC in Miami, FL for AMS 14 C dating. To avoid possible contamination, we carefully selected dating materials, collected them directly from the core, and avoided all possible root materials. The 14 C geochronology of the core was calculated in calendar years BP using Clam v2.2, cc4 = "mixed.14C" datasets (Blaauw, 2010) with

the regional reservoir offset of 200 (Törnqvist et al., 2015) (Fig. S3).

Sixty sediment samples were extracted at 1-cm internals from core LLWMA3 for 137 Cs and 210 Pb analyses. The samples were prepared following the methodology of Wilson and Allison (2008), and then counted for 24–48 h in a Canberra gamma(γ)-ray spectrometer. 137 Cs and 210 Pb activities were calculated following the methods in Allison et al. (2007), and reported in decays per minute per gram of dry sediment (dpm/g, 1 dpm = 60 Bq). The geochronology for the last 65 years is based on measurements of deposition of 137 Cs fallouts. The initiation of 137 Cs fallout is identified as 1954 CE and the maximum peak (in the northern hemisphere) as 1963 CE. The geochronology, developed on Clam v2.2 (Blaauw, 2010), incorporates both the radiocarbon and the gamma-ray data.

3.3. X-ray fluorescence

Geochemical analysis facilitates detecting hydro- and geochemical-conditions. An Innov-X Delta Premium DP-4000 X-ray fluorescence (XRF) analyzer was used to scan the length of core LLWMA3 at 2-cm intervals, detecting concentrations (ppm) of 32 elements (Ryu et al., 2022a), as calibrated with NIST standards 2710a and 2711a. Elemental ratios are increasingly being used (Ryu et al., 2018, 2022b) to infer the provenance of deposited sediments, and/or detect the influence of various background parameters. Here we use Ca/Rb as a proxy for Biogenic, Zr/Rb, Ti/Rb, K/Ti for Terrestrial; Ba for Marine; Mn/Rb, S/Rb for Minerogenic; and Br for Organic influence/origin of sediments, as detailed in Discussion.

3.4. Microfossil analysis

Sixty samples (1.8 ml each) were taken from core LLWMA3 at 5cm intervals for the counting of pollen, fungal spores (Glomus, Tetraploa, Pteridophytes), and charcoal fragments >10 μm. The samples were treated with a solution of 10% hydrochloric acid (HCl), 10% potassium hydroxide (KOH), and 49% hydrofluoric acid (HF) to remove calcium carbonate, break down organic molecules, and dissolve silicates (Liu et al., 2008), with exotic Lycopodium tablets added to each sample to determine pollen concentration (Stockmarr, 1971). At least 300 pollen grains were counted for each sample. Pollen identification was guided by published works (Wodehouse, 1937; Faegri et al., 1989; Willard et al., 2004; Ryu et al., 2022b). In order to distinguish Spartina pollen from other common wetland Poaceae plants such as Phragmites we carefully analyzed pollen morphology based on size and pore diameter. Spartina pollen is generally larger (maximum dimension 33.0-42.0 µm) than Phragmites pollen (maximum dimension between 21.9 and 26.5 µm), and has a larger pore (pore diameter of 3.8 µm versus 1.5–2.4 µm for Phragmites) (Willard et al., 2004). Foraminifera tests and dinoflagellates were analyzed to identify possible marine incursion using conventional methods (Boonstra et al., 2015). The pollen diagram was graphed with C2 software (Juggins, 2007) and Illustrator.

3.5. Species richness and diversity

Palynology-based diversity analysis was conducted using the software R package, "iNEXT (iNterpolation and EXTrapolation)" (Chao et al., 2020): producing coverage- and sample-size-based asymptotic & non-asymptotic analyses based on Hill numbers. "iNEXT" was used to calculate three measures of Hill numbers of species richness (q=0), Shannon diversity (q=1), and Simpson diversity (q=2), as a means of determining abundance (Chao et al., 2015). The unified coverage- and sample-size-based curves infer diversities in terms of species richness and true diversity via rarefaction and extrapolation (Chao et al., 2020) of different

communities with different sample sizes. Our datasets consist of 13,068 pollen-spore specimens with a matrix of fifty taxa and forty-eight variables. The best taxonomic resolution was selected based on the previous palynological studies (Rodrigues et al., 2021; Ryu et al., 2021b, 2022b). The analytical details concerning the asymptotic diversity model describing entire sample assemblages and the non-asymptotic diversity analysis for standardized sample coverage (completeness) are published in previous studies (Chao et al., 2015, 2020). The X-axis represents the sample size and the Y-axis indicates diversity, incorporating relative species richness in different time frames (zonation). A bootstrap method computes the 95% confidence intervals (shaded regions) (Chao et al., 2014).

3.6. Statistical analysis

Various R software packages (e.g., "factoextra", "FactoMineR", "ggplot") were used to identify the relative importance of various external mechanisms and biostratigraphic zones (e.g., zones 1–2, 2–3, 3–4, 4–5, 5–6) as a means of the multivariate statistical analyses, including principal component analysis (PCA) with a squared cosine function, estimating the representation of variables for a given observation, and constrained single-link cluster analysis (Ryu et al., 2022a). PCA biplots for the zone shifts compare ecological and geochemical datasets with ecosystem clusters (interdistributary, hydrophyte, mesophyte, *Typha* marsh, intermediate, and brackish), with confidence ellipses centered at the mean points of each ecosystem and display correlation values between two environments as the factors driving the first two components.

3.7. Geochemical proxies

The geochemical composition of coastal sediments results from a variety of factors, such as origin, type, amount, and frequency of discharge of the source water, oceanic transgression, vegetation, and microbial activities, all of which potentially leave detectable sedimentary signatures, which can be used to identify environmental conditions at the time of deposition. In this study, we employ elemental concentrations and ratios as proxies for biogenic (Ca/Rb), terrestrial (Zr/Rb, Ti/Rb, K/Ti), marine (Ba), minerogenic (Mn/Rb, S/Rb), and organic (Br) signatures in order to infer the source of sedimentary materials and the associated depositional mechanisms. Because rubidium (Rb) is widely distributed in rockforming minerals such as biotite, muscovite, feldspar, and illite (Rothwell and Croudace, 2015), it is present in large quantities in detrital mineral material and can be used as an elemental divisor for normalizing other conservative elements (Löwemark et al., 2011). Because calcium (Ca) in coastal environments generally originates as foraminiferal or molluscan calcite deposits, the Ca/Rb ratio indicates the level of biogenic calcite input (Hodell et al., 2008). Since zirconium (Zr) derives from quartz or coarse-grained granite, the Zr/Rb ratio can be used as a grain-size proxy. At our study site higher values, indicative of coarser grains, likely correlate with increased fluvial delivery (Wang et al., 2011). Because titanium (Ti) is a common component of metamorphic and igneous rocks, and is highly resistant to diagenetic processes, the level of titanium in riverine sediments is positively correlated with the deposition of fluvially-delivered allochthonous sediments (Buechakd, 1925), in our case, coarse-grained minerals such as laterites and bauxites from the lower Mississippi River basin (Buechakd, 1925). Hence, Ti/ Rb ratio represents terrestrial sediment fluxes delivered fluvially. Potassium (K), often occurring as potassium mica, or potassium feldspar, is a common constituent of igneous rocks. As an alkali metal, it behaves much like rubidium in estuarine environments, with high concentrations indicating fluvial activity (Culligan et al.,

2022), and a large K/Ti ratio indicating light-grained riverine minerals (e.g., illite). Barium (Ba) is highly reactive chemically, and never occurs as a free element in nature, but commonly is present in barite, widespread oceanic minerals such as barium sulfate (BaSO₄) and witherite (BaCO₃) (Sternberg et al., 2005), while its occurrence on land generally derives from mined deposits, or relict coarse sands that fail to escape from enclosed bay environments (Shaw et al., 1998). The presence of Ba is associated with coarsegrained sediments, and high concentrations generally indicate marine influence. Manganese (Mn) occurs in a variety of minerals, usually coupled with oxygen, silicate, and carbonates, occurring in nutrient- or toxicant-rich wetlands (Donahoe et al., 1994). Anoxic conditions resulting from flooding and waterlogging result in a high concentration of soluble manganese (Wang et al., 2021) as manganese leaches downward in a damp environment. Hence, in wetlands, the Mn/Rb ratio can be used to identify anoxic conditions resulting from increasing water depth (Ryu et al., 2018). Sulfur (S) is a key element in the biogeochemical recycling process (Pester et al., 2012). Although sulfur naturally occurs as reduced inorganic sulfur, organic sulfur (Org-S), or sulfate (SO_4^{2-}), the sulfur concentration in wetlands is tightly correlated with water-dissolved organic C concentrations (Burton et al., 2011) as carbon-bonded sulfur decomposes to Org-S, while Org-S converts to sulfate by hydrolysis (Chen et al., 2020). Because decomposition processes commonly result in the coupling of water-soluble sulfate coupling with Fe (Burton et al., 2011), in sediments, a high S/Rb ratio indicates reducing conditions. Bromine (Br) concentration is widely used in environmental studies as a proxy for biomass, as Br strongly combines with organic material to form bromo-organic compounds (Ryu et al., 2018). These elemental concentrations and ratios are used as proxies for biogenic, terrestrial, marine, minerogenic, and organic signatures to facilitate the identification of the hydrological and geological conditions that prevailed during the time of deposition. Additionally, elevated levels of Glomus, a arbuscular mycorrhiza, can serve as a proxy for soil erosion and flooding (Van Geel et al., 1989, 2003).

4. Results

4.1. Sediment stratigraphy

We identify six stratigraphic zones, with the three topmost zones (6, 5, 4) occurring in all three cores, and the bottom three zones (3, 2, 1) occurring in the long core LLWMA3 (Fig. 2). Zone 1 (487-290 cm) shows upward coarsening as interstratified lightgrey silts/clays (487-375 cm) shift to interbedded fine sands/silts with planar lamination from 375 to 290 cm. Water content is 20–52%, organics 1–10%, carbonates 2–4%, and residual (mainly silicates) 80–96%.

Zone 2 (290-220 cm) has a bottom section (290-280 cm) of alternating fine-sand and light-grey silt with planar lamination. Organic-rich sediments consisting of dark-brown and black peats occur from 280 to 220 cm, with grey clays embedded at 262, 257, and 253 cm. Water content is 36–85%, organics 5–73%, carbonates 1–7%, and residual 21–94%.

Zone 3 (220-164 cm) exhibits alternating black muds with embedded plant debris (stems, roots) and light-grey silt/clay, with the black clays presenting at 227–210, 205–197, 193–190, 185-170 cm. Water content is 30–77%, organics 3–44%, carbonates 1–5%, and residual up to 95%.

Zone 4 (164-77 cm) consists of alternating light-grey silts (160-157, 150-145, 140-136, 135-132, 120-112, 105-99, 95-93 cm) and brown to black clays. The water (37-78%), organics (4-36%), carbonate (0-3%), and silicates (46-94%) percentages

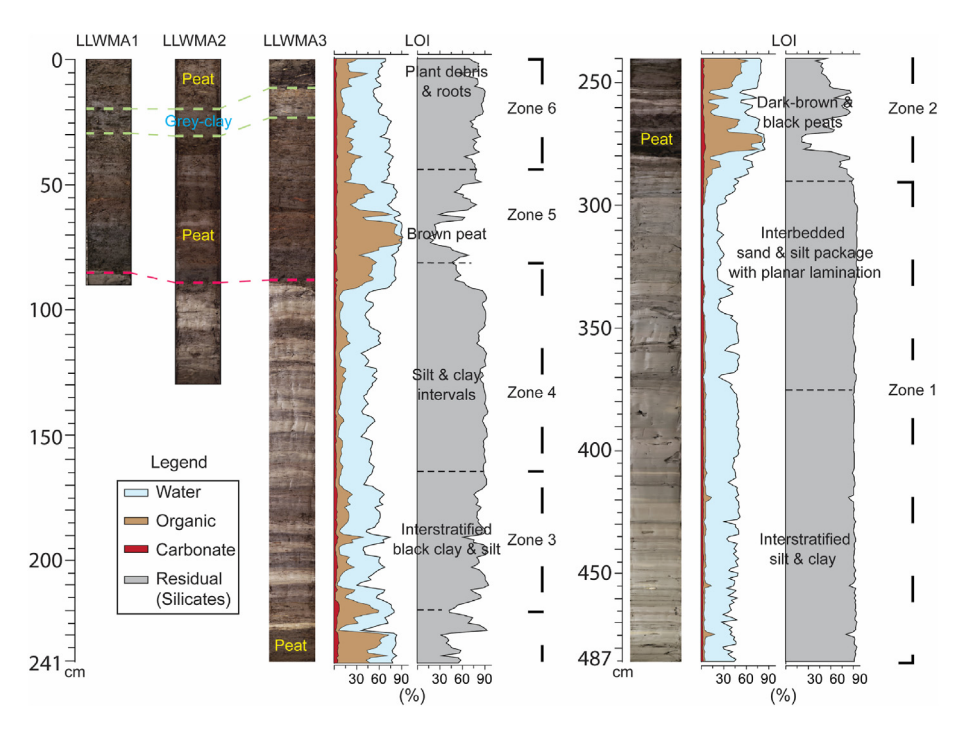


Fig. 2. Stratigraphic profiles of LLWMA1, LLWMA2, LLWMA3 showing six stratigraphic facies and sedimentary characteristics. LOI results and sediment types are displayed.

fluctuate in concert with the silt-clay alternations. Plant debris is embedded in the grey silt deposits. A black clay package with high organics (up to 52%) and water (76–86%) occurs at 89-77 cm.

Zone 5 (77-44 cm) is mainly peat. Roots and stems are embedded in brown peats with high water (63–91%) and organic (up to 82%) percentages. A mineral layer presents at 50 cm as silicates increase up to 86%. Water content is 12–82%, carbonates 1–4%, organics 12–82%, and residual 14–85%.

Zone 6 (44-0 cm) shows increasing percentages of water (52–80%) and silicates (57–91%) with heavy loads of plant roots. Light-grey clays at 18-13 cm contain 7–9% organics, 53–58% water, and <2% carbonate contents, while black clay layers (8-7 cm) exhibit a rapid increase in organics (up to 39%) and water (59–60%) percentages. The top 10 cm is predominately intact roots. Water content is 52–80%, organics 7–39%, carbonates 1–4%, and residuals 57–91%.

4.2. Chronology

Organic materials (plant debris) extracted from LLWMA3 at 464, 292, 230, 173, and 92 cm yielded calibrated radiocarbon dates of 3049 ± 92 , 2332 ± 91 , 1523 ± 89 , 970 ± 60 , and 551 ± 57 yrs BP, respectively (Table S2). These dates are highly correlated with the active periods of St. Bernard subdelta lobe 7 (Fig. S1.1) and Lafourche subdelta lobe 10 (Fig. S1.2).

The radiochemical analyses mark the initiation of 137 Cs activity at 54 cm (1954 CE), and the peak at 51 cm (1963 CE). The 210 Pb $_{xs}$ activities are erratic, showing no notable logarithmical decrease (Fig. S1.2), likely due to activity levels varying with sediment types, increasing in clay minerals and degraded litter/high organics, while decreasing in coarser material. As a result, the 210 Pb $_{xs}$ data was not used in creating the age-depth linear interpolation curve. The age-depth model (Fig. S3) shows the five calibrated 14 C dates with a 95% probability for gaussian distribution displayed as a grey shadow. The sediment accumulation rate (SAR) for the period of 1963–2018, calculated from the 137 Cs peak, is 0.9 cm/yr. Due to the lack of

notable logarithmical decrease in the $^{210}\text{Pb}_{xs}$ activity, the $^{210}\text{Pb}_{x}$ SAR was not applied.

4.3. X-ray fluorescence (XRF)

In this study, simple elemental ratios are used (Fig. 3) as proxies to infer the biogenic (Ca/Rb), terrestrial (Zr/Rb, Ti/Rb, K/Ti), marine (Ba), minerogenic (Mn/Rb, S/Rb), and organic (Br) source/environmental background of deposited sediments, as detailed in Discussion, section 3.1. Zone 1 is characterized by enhanced influxes of terrestrial elements. The Zr/Rb and Ti/Rb ratios increase toward the zone-top. Episodic spikes of the Zr/Rb ratio correlate with sand packages between 371 and 307 cm. The Ca/Rb ratio increases above 400 cm, concordant with elevated Ba concentrations. Periodic peaks of Mn/Rb ratio correspond to organic clays throughout the zone. Zone 2 displays elevated Br concentrations coupled with organic-rich sediments throughout the zone. Episodic spikes of Ca, Mn, and S/Rb are associated with high organic contents (up to 73%). The Zr/Rb and Ti/Rb ratios are relatively low. Zone 3 displays a small increase in the Zr/Rb and Ti/Rb ratios. Periodic Br spikes correspond to elevated Mn/Rb levels and organic clays. The Ti/Rb ratio continues to increase throughout zones 3 and 4, while rapidly decreasing at the boundary between zones 4 and 5, coupled with rapid increases in organic percentages and elevated Br. Zone 4 shows generally stable levels for most ratios and Br. Zone 5 shows a sharp decrease in terrestrial elements, followed by rapid increases in Ti, K, Mn/Rb, and the episodic spikes of the S/Rb ratio. Zone 6 displays generally stable ratios below 20 cm, followed by a rapid decrease in the Ca/Rb ratio. Increases in the Ti/Rb and K/Ti ratios correspond to low organic contents in the light-grey muds at 16 cm. Elevated Br concentration and Ti, Ca, and Mn/Rb ratios are associated with increased organic content in the top 6 cm.

4.4. Microfossil analysis

A total of 40 pollen taxa and spores (Glomus, Tetraploa,

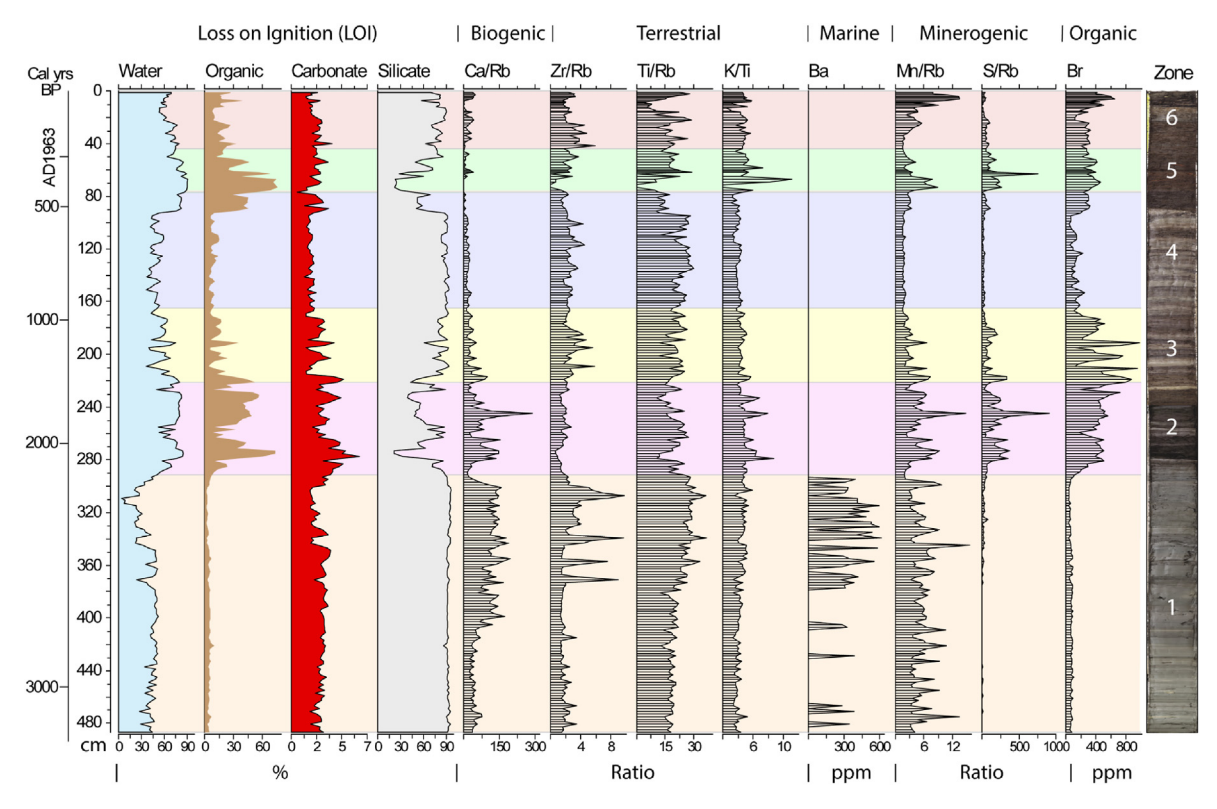


Fig. 3. LOI and geochemistry data. Percentages of water, organic, carbonate, and silicate content, and geochemical profiles of biogenic, terrestrial, marine, minerogenic, and organic are displayed.

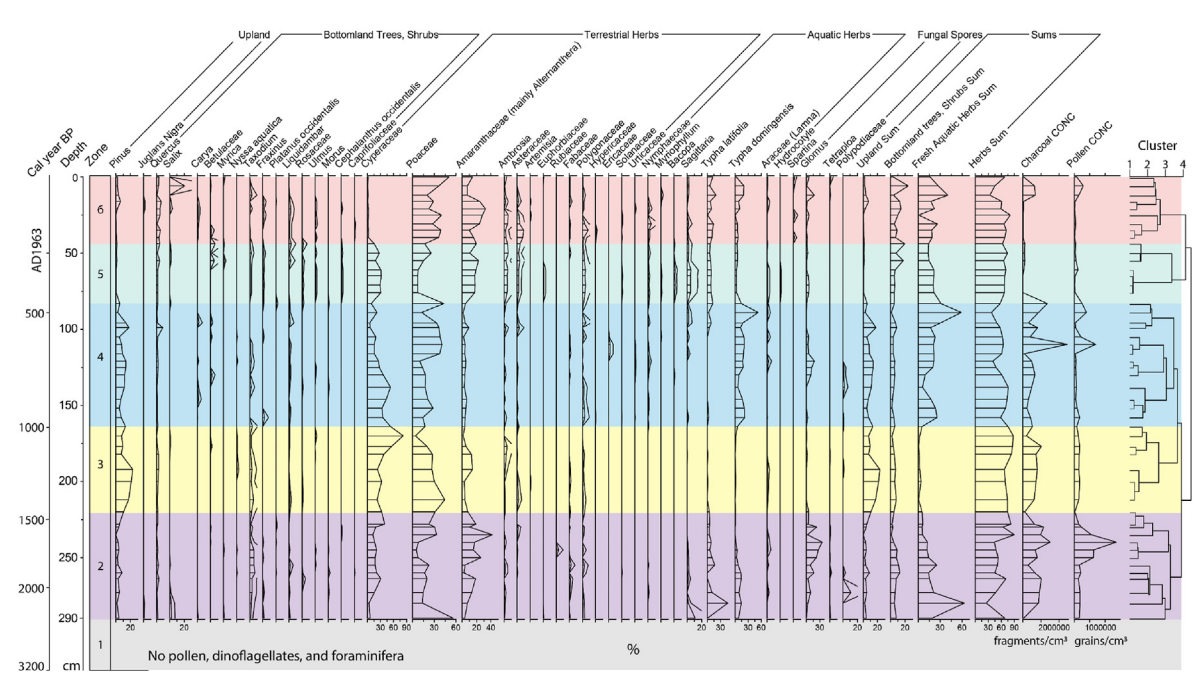


Fig. 4. Pollen percentage diagram. Forty (40) pollen taxa, and three spores corresponding to at least 1% of the sum are shown. Cluster analysis was used to distinguish zones. Charcoal and pollen concentrations are graphed as grains per cubic centimeter and fragments per cubic centimeter, respectively. Unshaded curves represent the 3 × exaggeration, except high percentage pollen taxa (*Pinus*, *Quercus*, Cyperaceae, Poaceae, Amaranthaceae, *Typha*). Since pollen was absent throughout the zone 1 and no spores, dinoflagellates, and foraminifera were detected, we omit zone 1.

Polypodiaceae) were counted to elucidate the changes in the vegetation cover over the length of the core (Fig. 4). The highest maximum percentage of each major taxa for each zone is presented in Table S3. Pollen was absent throughout zone 1 and no spores,

dinoflagellates, and foraminifera were detected, except an intact shell (*Rangia cuneata* at 481 cm) and shell fragments at 455 cm. Zone 2 is characterized by a transition from aquatic herbs (Araceae, *Sagittaria*, and *Typha*) at the bottom of the zone to terrestrial herbs

(e.g., Amaranthaceae: mainly Alternanthera, Ambrosia, Fabaceae, Polygonaceae, Rubiaceae) ~ 250 cm. Arboreal pollen taxa including Pinus, Quercus, Taxodium, and Liquidambar. Spores (Glomus, Polypodiaceae) are abundant between 260 and 220 cm. Zone 3 is represented by a mesophytic community as terrestrial herbs continue to increase throughout the zone, including Cyperaceae, Poaceae, Amaranthaceae: mainly Alternanthera, Ambrosia, and Asteraceae. Zone 3 exhibits highly diverse vegetation with high percentages of trees (Pinus, Quercus, Liquidambar) and terrestrial herbs and low percentages of aquatic (Sagittaria, Araceae) herbs throughout the zone. In zone 4 the percentages of Cyperaceae steadily decrease, while aquatic herbs (Typha, Sagittaria, Araceae: mainly Lamna) continue to increase toward the top of the zone. Microcharcoal concentrations increase at 110-83 cm where dark clay occurs, along with increased pollen concentrations. The abundance of Typha rapidly decreases in zone 5, while aquatic herbs (Sagittaria, Araceae) and flowering plants (Amaranthaceae: mainly Alternanthera, Ambrosia, Asteraceae, Euphorbiaceae, Polygonaceae) increase throughout the zone. In zone 5, the percentages of arboreal taxa are relatively low (~6.7%), while various herbs were identified. Cyperaceae shows a sharp decrease in zone 6, while first grasses (Poaceae) and flowering plants (Amaranthaceae: mainly Alternanthera, Ambrosia, Asteraceae) increase, followed by high percentages of aquatic plants (Typha). Juglans is present in the light-grey clays at 18-13 cm. Flowering plant taxa such as Ambrosia, Asteraceae, and Polygonaceae rapidly decrease above 20 cm. Low percentages of Spartina (0-2%) were identified at 40, 25, and 1 cm.

4.5. Species diversity

Palynology-based biodiversity models are used to evaluate sample completeness, asymptotic diversity estimates (true diversity), and coverage-based rarefaction and extrapolation, thereby quantitatively accessing species richness and diversity for each zone based on Hill numbers (Hsieh et al., 2016). The rarefied curves indicate diversity values (solid-line) and empirical diversity profiles (dotted-line) for each zone (Fig. 5). An assessment of sample completeness profiles displaying the estimated sample completeness in terms of q = 0 (species richness), q = 1 (Shannon diversity), and q = 2 (Simpson diversity), displays an increase in sample completeness throughout the zones (Fig. 5-a). The estimated sample-completeness (SC) is generally similar across the zones, as the sample coverage values range from 87 to 95% (Table S4). Size-based rarefaction and extrapolation profiles (when q = 0) illustrate increasing richness curves on the X-axis, extrapolated (dashed lines) almost double the reference sample size. Shannon (when q = 1) and Simpson (when q = 2) diversity models show a diversity variation from high to low in zones 3, 2, 6, 4, and 5, respectively, with the estimation of undetected diversity values of 0.08–1.23 (except for zone 3 with a value of 3.8). The standardized coverage-based diversity values vary between zones: 93% (zone 2), 87% (zone 3), 95% (zone 4), 95% (zone 5), 94% (zone 6) (Fig. 5-c). Of the palynology-based biodiversity estimation, the species richness continues to rise (double the reference sample size), while coverage-based rarefaction and extrapolation with Hill numbers capture the true diversity within each ecological zone.

4.6. Statistical analysis

Multivariate statistical analysis elucidates the relationships between ecological and geochemical signatures and the underlying ecosystem clusters (Fig. 6). PCA biplots were constructed for all five zone shifts in order to accentuate the changes in depositional environments occurring across zones. In all five transitions, the two

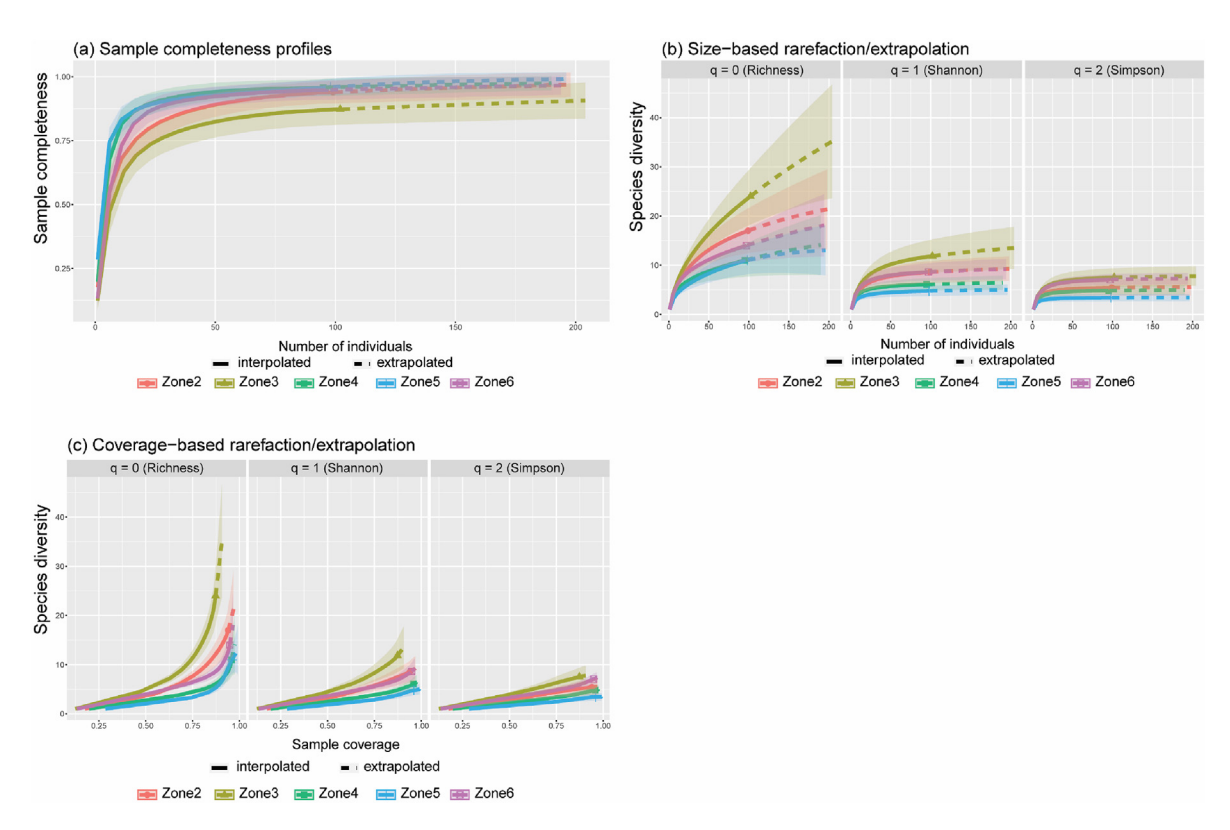


Fig. 5. Palynology-based diversity analysis. Figure displays (a) sample-completeness profiles, (b) size-based rarefaction and extrapolation curves, and (c) coverage-based rarefaction and extrapolation curves. The curves with interpolated (solid lines) and extrapolation (dotted lines) are displayed with 95% confidence intervals marked as shaded areas). Note: since there is no pollen present in zone 1, we omit zone 1.

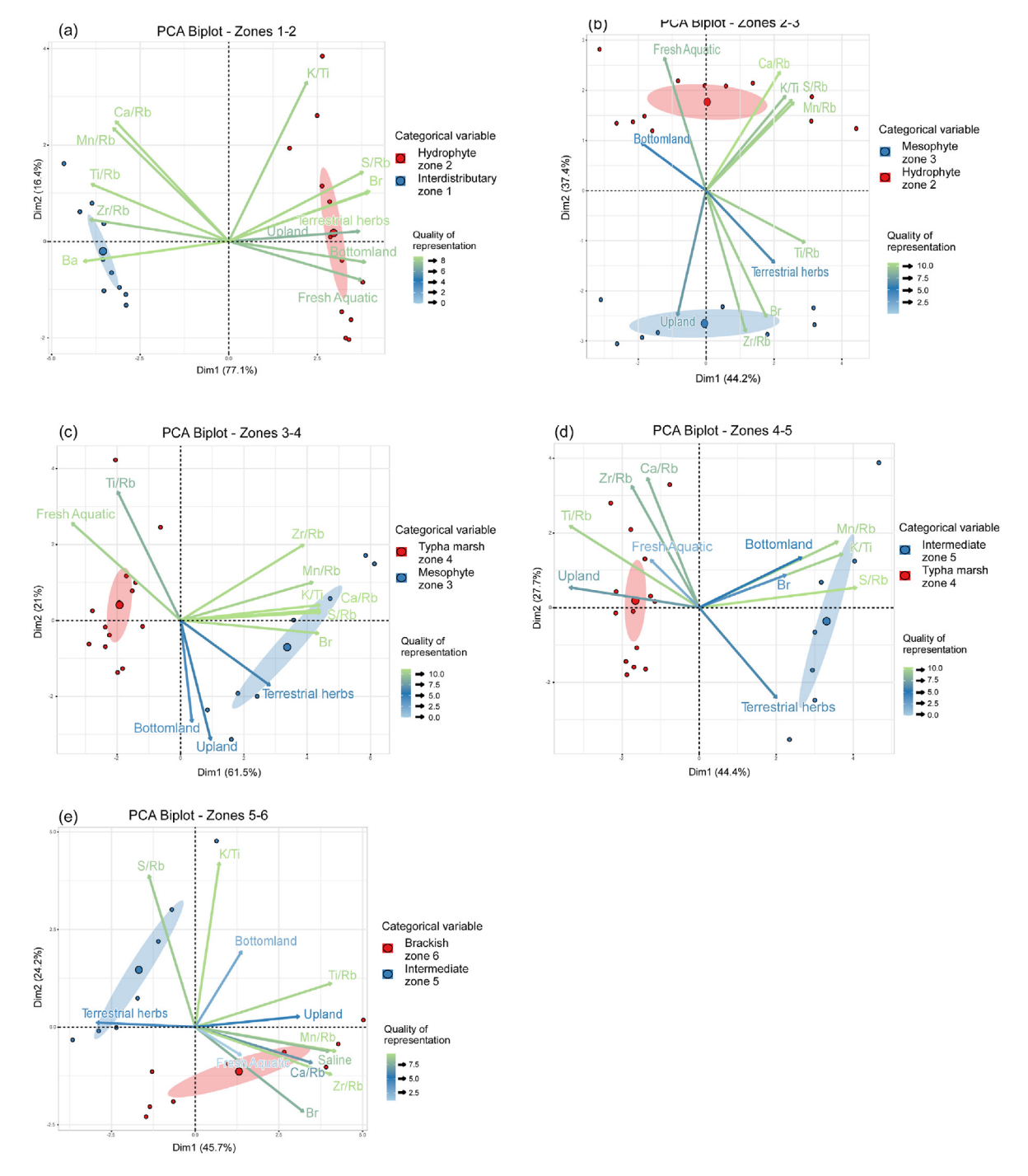


Fig. 6. PCA-plots displaying six ecosystem clusters (interdistributary, hydrophytic marsh, mesophytic prairie, *Typha* marsh, intermediate marsh, and brackish marsh) and distance matrices for ecological (Upland trees, Bottomland hardwoods, Terrestrial herbs, Fresh aquatic herbs) and geochemical variables (Ca/Rb, Zr/Rb, Ti/Rb, K/Ti, Ba, Mn/Rb, S/Rb, Br) compared between zones. The contributions of variables in accounting for the variability in a given principal component are expressed in percentages.

zones are widely separated in coordination space, with the important components consisting of contrasting sets of variables. For these shifts, the first principal components (the Dim 1 axis) account for 44.2–77.1% of the total variance, and the second principal components (the Dim 2 axis) account for 16.4–37.4%, indicating that combined, the differences between zones are almost completely explained by the variables driving the first two components. The PCA-biplot for the zone 1–2 shift displays high correlations between interdistributary variables and terrestrial proxies (Zr/Rb, Ti/Rb) (zone 1), while the hydrophyte clusters (zone 2) are

strongly correlated with trees, herbs, and the minerogenic (S/Rb) and organic (Br) proxies (Fig. 6a). The variables for zones 2–3 transition are latitudinally scattered with the hydrophyte cluster is associated with freshwater aquatic herbs (fresh aquatic) (zone 2), with the minerogenic and biogenic variables showing positive loadings on the first quadrant, positively correlated with K/Ti, while the mesophyte cluster (zone 3) correlates with upland, Zr/Rb, and Br (Fig. 6b). The PCA-biplot for the zones 3–4 transition (Fig. 6c) shows the mesophyte cluster (zone 3) strongly correlating with the terrestrial, minerogenic, and organic proxies, while a positive

correlation occurs between *Typha* marsh and freshwater aquatic herbs with the Ti/Rb in the second quadrant for zone 4. At the zones 4–5 transition, the *Typha* marsh (zone 4) and intermediate cluster (zone 5) are separated along the X-axis as Ti/Rb, Zr/Rb, and Ca/Rb are correlated with freshwater aquatic herbs and upland trees in the second quadrant, while the intermediate cluster is tightly associated with the Mn/Rb, S/Rb, and K/Ti (Fig. 6d). The brackish marsh (zone 6) is represented by increasing salinity, correlated with the brackish cluster in the fourth quadrant, while the intermediate cluster (zone 5) is highly associated with the S/Rb (Fig. 6e).

5. Discussion

5.1. Paleoecological reconstruction

5.1.1. Zone 1 (3200–2300 BP) interdistributary-bay

The interstratified silt and clay with planar lamination indicate that coarse- and fine-grained sediments were carried through crevasse splays into an open water bay formed in the space between prograding distributaries (Fig. 7). The intact shell (Rangia cuneata) deposited around 3200 BP (481 cm) implies a brackish environment. Although Rangia cuneata occurs across a range of salinities, from intermediate to the open ocean, it reproduces best in brackish environments (Cobb et al., 2009). The episodic spikes of Ba represent sporadic intrusions of higher salinity water into the bay, while strong terrestrial value indicates increasing progradation and fluvial discharge. The variations of biogenic and terrestrial proxies suggest an enclosed, relatively calm bay until ~2700 BP. The sedimentary input was mainly terrestrial, marked by high Ti, with intermittent marine input marked by elevated Ba concentrations. Ca/Rb and Zr/Rb spikes indicate that increasing fluvial activities (e.g., crevasse splays) likely reworked and redistributed detrital carbonate clays during a period of delta progradation. During the deltaic cycle, compaction of unconsolidated sediments allows for frequent saltwater intrusion, while enlarged accommodation space leads to the reoccupation of river channels and deposition of terrestrial sediments, as marked by high Zr/Rb, Ti/Rb, and Mn/Rb ratios. The interbedded upward-coarsening and thickening sand and silt packages with planar lamination indicate progradational deposits ~2500 BP as the St. Bernard subdelta (Bayou des Families) developed around the study site (Fig. 1) (Saucier, 1968; Levin, 1990; Ryu et al., 2021b).

5.1.2. Zone 2 (2300–1420 BP) hydrophytic freshwater marsh Delta progradation led to a changing environment ~ 2300 BP,

including both marshes and small cypress patches, as evidenced by the increase in pollen concentrations of bottomland trees and shrubs, and terrestrial and aquatic herbs. This resulted in the deposition of organic-rich sediments, marked by elevated Br concentrations and an increased number of plant taxa. The hydrophytic freshwater vegetation likely colonized saturated soils along the distributary channels, while small patches of Taxodium-Nyssa swamp developed in back swamps. During delta growth, river meanders generally increase the number of environmental types (e.g., oxbow lakes, levees, and point bars) (Saucier, 1968), and conjointly, ecosystem diversification. The increase in various herbaceous taxa indicates an expansion of marshlands ~2000 BP. The presence of aquatic plants such as Sagittaria, Typha latifolia, and Araceae (*Lemna*) imply saturated soil conditions that lasted several centuries. Episodic spikes of Mn/Rb and S/Rb coupled with high percentages of Araceae (mainly Lemna) and arbuscular mycorrhizal (Glomus), indicative of soil erosion (Van Geel et al., 1989, 2003) ~ 1700 BP, suggest frequent fluvial local floods (Cox, 1983; Ryu et al., 2022b), with the increase in sulfur and manganese concentrations indicating anoxic conditions caused by prolonged inundation. The elevated Ca/Rb ratio may have resulted from fluvial flood events resuspending and redepositing detrital carbonates.

5.1.3. Zone 3 (1420-920 BP) mesophytic coastal prairie

The interstratified black clays and silts coupled with an increase in mesophytic arboreal- and non-arboreal pollen taxa indicate the increased influence of terrestrial sources. The increases in the K/Ti ratio, Br concentration, and the number of flowering herbs and trees taxa imply increasingly diverse vegetation, including both aquatic (*Typha*) and dryland plants (*Ambrosia*, Asteraceae, Fabaceae, and Polygonaceae). The presence of such plants as *Pinus*, *Juglans*, *Liquidambar*, and *Ulmus* suggests the presence of higher, dryer areas, such as natural levees along river channels. Episodic spikes of terrestrial proxies (Zr/Rb, Ti/Rb) coupled with fine-to coarse-silts suggest fluvially driven clastic deposition between 1300—1000 BP, associated with the extension of the Lafourche Delta (Bayou Lafourche), a chronological match with previous studies (Saucier, 1968; Chamberlain et al., 2018; Ryu et al., 2021b) (Fig. 1).

5.1.4. Zone 4 (920–330 BP) Freshwater Typha marsh

The increase in light-grey silt and clay intervals coupled with a rapid increase in *Typha* (*T. domingensis* and *T. latifolia*) and Araceae (mainly *Lemna*) taxa indicate a transition to a *Typha*-dominated freshwater ecosystem ~ 900 BP (Fig. 8). *Typha* mainly occurs in locations with salinity from 0.3 to 5.5 ppt (Visser et al., 2013). The

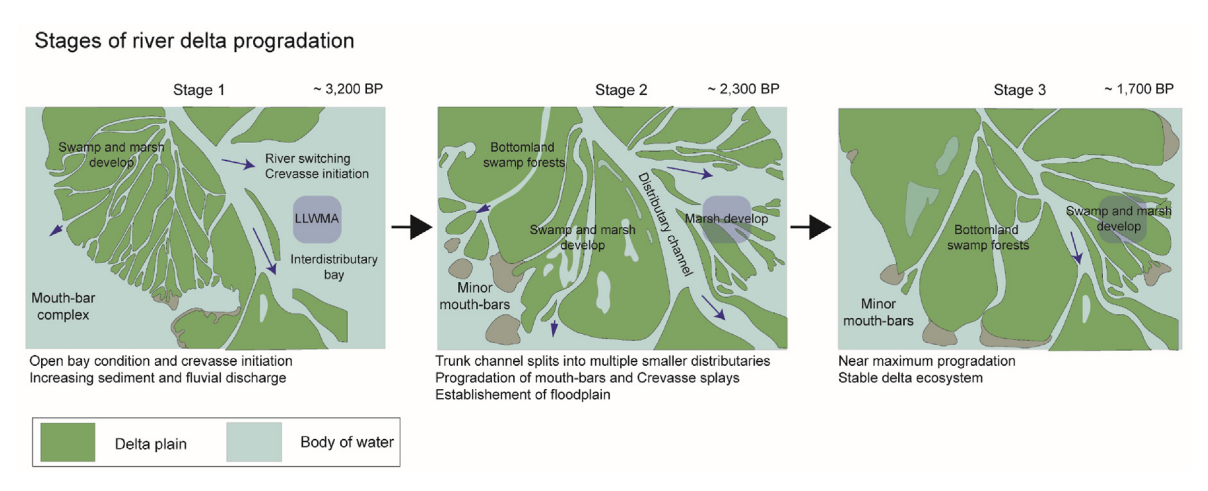


Fig. 7. Conceptual model of interdistributary bay evolution associated with delta progradation and ecosystem development.

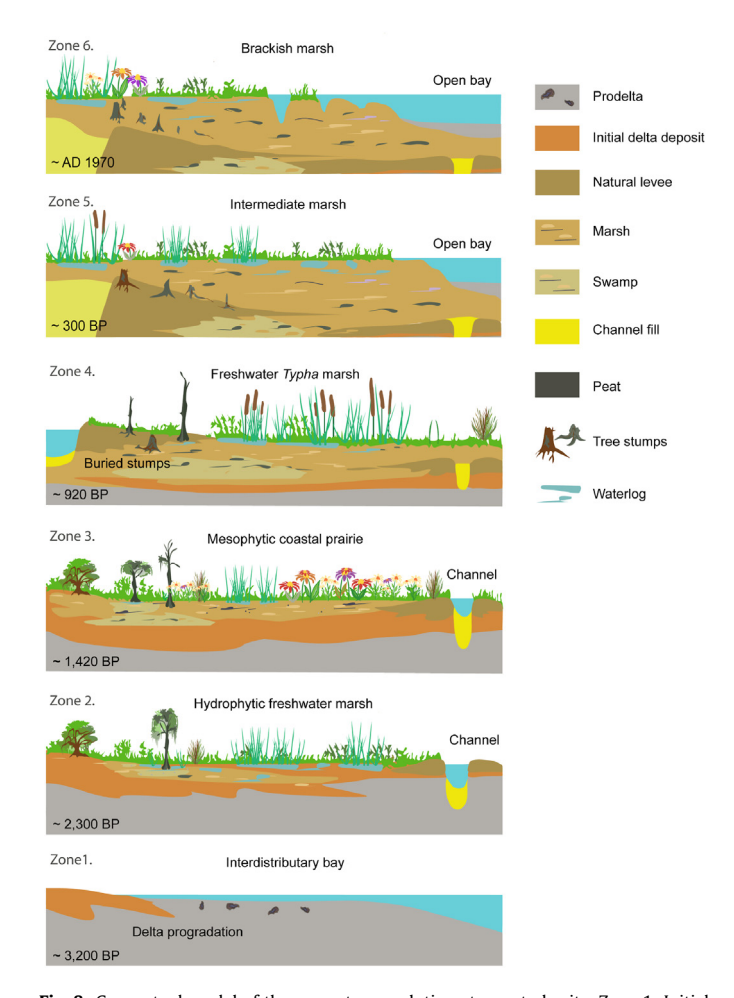


Fig. 8. Conceptual model of the ecosystem evolution at our study site. Zone 1: Initial delta plain develops over interdistributary bay, with strong fluvial discharge. Zone 2: Increased freshwater and sediments lead to an establishment of hydrophytic freshwater marsh plants and small patches of bottomland trees in water logged areas. Zone 3: Diverse freshwater mesophytic coastal prairie, with the number of upland and bottomland trees across in a more heterogenic topography (e.g., levee and meander cutoff). Zone 4: The Lafourche subdelta progradation results in the development of *Typha* dominant marsh. Zone 5: As the lobe is abandoned, reduced terrestrial flux leads to subsidence and erosion and the rapid decline of the *Typha* community, which transitions to intermediate marsh. Zone 6: The intermediate marsh erodes due to RSLR and reduced sediment supply, transitioning to a brackish marsh.

small increase in the terrestrial proxy (Ti/Rb) likely results from the transportation of terrestrial materials by the Lafourche subdelta (Bayou Lafourche), which was in progradation (Chamberlain et al., 2018). Around 700 BP a significant vegetative change took place, as Typha, Sagittaria, and Poaceae (e.g., Paspalum) began replacing Cyperaceae (e.g., Schoenoplectus, Cyperus), implying a shift from coastal prairie (mid-to tall-grass and sedges) to an intermediate hydrophytic ecosystem (mid-to short-grasses with Typha patches). This was likely an effect of the Mississippi River diverting into the Plaguemines and Balize Deltas (Fig. 1), as the Lafourche Delta began transgressing after 600 BP (Chamberlain et al., 2018), reducing terrestrial materials. During this period the movements of the lobes of St. Bernard, Lafourche, and Plaquemines and Balize deltas were spatially and temporally variable. Saturated soil conditions likely persisted for several centuries, with the mud and clastic intervals formed in those depressions with sufficient water to support vegetation. Afterward, a significant decrease in terrestrial elements (Ti, Zr) occurred around 400 BP, suggesting a rapid decrease in terrestrial flux (water and sediment).

5.1.5. Zone 5 (330 CE) transition to intermediate marsh

The transgressive phase of the Lafourche subdelta reduced fluvial flux over the study site and led to an increase in autochthonous sediment source (peat) after 330 BP, as Bayou Lafourche was almost entirely abandoned as the main distributary shifted eastward (Plaguemines and Balize deltas). The elevated Mn/Rb ratio indicates subsequent subsidence with the high K/Ti ratio suggesting that terrestrial materials filled the sunken grounds during precipitation events. The episodic spikes of the S/Rb ratio indicate anoxic environments ~100 BP as the terrestrial input reduced beyond the threshold necessary to support the wetlands as indicated by a rapid decrease in Typha abundance and pollen concentrations. The reduced fluvial flux led to a lowering of the water table and the decomposition of peat and created a patchwork of potholes over the marsh, as evidenced by the increase in the S/Rb and Mn/Rb ratios. During the transgressive phase, the site became more vulnerable to large meteorological events such as floods and hurricane-generated storm surges, as evidenced by clastic deposits at 1965 CE (Ryu et al., 2018), and a slight increase in the Ca/Rb ratio toward the top of the zone.

5.1.6. Zone 6 (1972 CE - present) brackish marsh

After 1972 CE the episodic spikes of *Spartina* pollen, and intact grass stems (paspalum) and common reed (Phragmites) roots embedded in light-grey clays coupled with high Br concentrations indicate a shift to a brackish marsh. RSL has been rising continuously over the last century, with rates as high as 0.23 cm/yr (Gornitz et al., 1982), driving a salinity increase (up to 8.5 ppt) after the 1900s (Banks et al., 2016). The damming of Bayou Lafourche in 1904 CE accelerated both the salinity increase and marsh retreat by reducing the influx of water and sediment. As a result of the coastal retreat hurricane-generated storm surges push saline water further inland, marked at our site by elevated concentrations of marine elements (Sr, Ca) (Fig. S4). The marsh restoration projects, consisting mainly of freshwater diversions, which began ~ AD 2000 around Barataria Bay, redirected large volumes of freshwater to the area (Day et al., 2016; Xu et al., 2019), and reversed the salinity increase, as evidenced by the increase in freshwater aquatic herbs (e.g., Typha, Araceae, and Myriophyllum) after 2000 CE.

5.1.7. Paleoenvironmental reconstruction summary; a sequence of six major ecosystems occurred at our study site since 3200 BP

- 1) Interdistributary-bay (3.2–2.3 cal kyr BP),
- 2) Hydrophytic freshwater marsh (2.3-1.42 cal kyr BP),
- 3) Mesophytic coastal prairie (1.42-0.92 cal kyr BP),
- 4) Freshwater *Typha* marsh (0.92–0.33 cal kyr BP),
- 5) Intermediate marsh (0.33 cal kyr BP 1972 CE),
- 6) Brackish marsh (1972 CE present).

5.2. Ecosystem diversity as related to delta cycle

Plant diversity and species richness levels were assessed for each zone using palynology-based diversity models, which evaluated sample completeness, asymptotic diversity (true diversity), and coverage-based species richness (Hsieh et al., 2016). The sample completeness curves show nearly complete samples for each zone, equally treated individual samples (Chao et al., 2020), as indicated by the slopes of curves approaching zero (Fig. 5a). Species richness and species diversity are highly correlated, with both having the highest values in zone 3, with the lowest diversity and richness occurring in zones 4 and 5 (Fig. 5b). This suggests a significant relationship between species diversity and the Mississippi delta cycle.

The effect of the delta cycle on species diversity is largely

irrelevant during zone 1, as no delta lobe is affecting the location. Zone 2 is contemporary with the progradation of the St Bernard lobe. During this period of progradation, species diversity increases as plant communities colonize the delta plain. After 2300 BP, both upland and bottomland trees, including Quercus, Carya, Betulaceae, Taxodium, Nyssa, Fraxinus, Platanus, and Liquidambar occur in the vicinity of the study site, likely along natural levees and back swamps, while flowering plants and grasses (Cyperaceae, Poaceae, Amaranthaceae: mainly Alternanthera, Ambrosia, Asteraceae, Polygonaceae, and Ericaceae) dominate the lower elevations. Over time, as sediments accumulated, the St Bernard Delta became hydrologically inefficient, and the Mississippi River changed course far upstream and began discharging to the southwest and the southeast. Increased diversity during this zone is possibly artificially amplified by the fluvial transport of exotic taxa from distant watersheds within the Mississippi basin, Chmura et al. (1999) show that distant pollen transported by the Mississippi typically consists of Pinus, Chenopodiaceae, and Amaranthaceae. Other taxa, readily transported from distant reaches of the Mississippi include Abies and Picea, which occur at higher elevations in the Missouri River watershed (Chen et al., 2000), and Tilia, Juniperus virginiana, Acer, Ostrya, and Carpinus, from more temperate sections of the Ontario and Ohio River drainage systems (Crowder and Cuddy, 1972). However, these taxa are not present, even in small concentrations, suggesting that the deposition of allochthonous pollen from distant locals is not occurring. The high concentrations of the locally occurring taxa, Quercus, Taxodium, Typha, and Cyperaceae, indicate that the local pollen overwhelms the far-field pollen within this zone, as does the overall assemblage which closely resembles that of the other zones. Although the possibility exists that some of the diversity increase is due to the presence of pollen from distant sources, we do not believe this to be a significant factor.

During zone 3, the abandoned channels subsided unevenly, while newly created multiple distributaries of the Lafourche subdelta (Bayou Lafourche), led to greater geomorphic heterogeneity (e.g., oxbow lakes, levees, and point bars), providing the necessary environmental settings for a wider spectrum of plant communities, including both upland and bottomland trees, and terrestrial and aquatic herbs. Indirect freshwater input or local runoff supported bottomland trees (*Taxodium*, *Liquidambar*), shrubs (*Rhus*), and flowering plants (Asteraceae) in the higher elevations, while freshwater hydrophytic and mesophytic herbs flourished in the lower elevations. The maximum ecosystem diversity occurred ~1000 BP.

During zones 4 and 5 the abatement of the delta progradation significantly reduced plant diversity. During this period the delta lobe subsided, and the input of terrestrial coarse material decreased, reducing the geomorphic heterogeneity. The study site, located in the distal portion of the Bayou Lafourche, received a minimal stream flow, resulting in saturated soil conditions and a significant increase in such hydrophytic plants as *Typha*, *Sagittaria*, and Araceae by 500 BP.

During zone 5, a significant decrease in terrestrial flux (both water and sediment) and the dewatering of the underlying sediments accelerated land subsidence, and consequently, a reduction in plant diversity. The sunken grounds, saturated during precipitation events, became anoxic, and thus unable to support the wetlands, as indicated by a rapid decrease in *Typha* abundance and pollen concentrations.

During Zone 6 landscape diversity was low, and no longer affected by the delta cycle. Instead, the rather homogeneous environment is a result of RSLR, resulting in erosion, the loss of habitat types, and contamination of soil with salt, as evidenced by the episodic spikes of *Spartina* pollen. The relatively higher plant diversity and increase in freshwater aquatic herbs (e.g., *Typha*,

Araceae, and *Myriophyllum*) after 2000 CE are likely due to the implementation of various marsh restoration projects (mainly freshwater diversions) in Barataria Bay.

Species diversity can be closely correlated to landscape heterogeneity, which rises and falls with the delta cycle. As a lobe forms, diversity increases along with the increase in water and sediment. Biological diversity then reaches a maximum during the period covering the transition from regression to transgression, correlating to the period of the maximum number of environmental settings. Eventually, the subsidence associated with transgression becomes general, thereby decreasing the topographical and hydrological diversity. This reduction in the number of environmental settings, coupled with reduced nutrient and freshwater input, results in a reduction in plant diversity and richness. Until a new lobe forms in the area, the delta cycle eventually becomes irrelevant and vegetation dynamics are controlled by other factors.

Some ambiguity/uncertainty possibly exists under this methodology, especially in the diversity level as the software was likely developed for Linnaean systems which are not isomorphic with the format of pollen taxonomy. Species diversity is not only dependent on species richness, the number of different species present in the area, but also on species evenness, as compared to the similarity of the population size of each of the species present. In addition, rarefaction curves provide information about whether enough samples have been collected (Chao et al., 2020).

5.3. Inferred drivers

With the unique chemical and ecological signatures, the PCA biplots (Ryu et al., 2022a) can help identify the processes controlling the depositional environment for each of the six zones (Fig. 6). The important geochemical variables in zone 1, the interdistributary bay, are the marine indicator Ba and the biogenic indicator Ca/Rb, and the elevated terrestrial indicators Zr/Rb and Ti/Rb, which increase near the top of the zone. This suggests a shift from marine to fluvial conditions, with an increase in the volume of freshwater and coarse terrestrial material (allochthonous sources) being transported into the subaqueous bay.

In the freshwater hydrophytic marsh (zone 2), the dominance of the terrestrial (K/Ti) and organic (Br) indicators imply that the fluvial delivery of fine terrestrial materials (silt, clay) associated with the delta progradation raised the land above water level, and increased soil organic content, resulting in an increase in plant abundance and diversity.

The mesophytic coastal prairie (zone 3), which occurred during the period of maximum delta development (: stage 3), is characterized by the terrestrial indicators (Ki/Ti, Zr/Rb), terrestrial herbs, and upland plants. This suggests that fluvial discharges of sediment and freshwater dominated a depositional environment which supported marsh ecosystems and increased plant diversity.

Zone 4, a freshwater *Typha* marsh, is marked by a shift from terrestrial to freshwater aquatic herbs and the lowered importance of several terrestrial indicators, indicating reduced fluvial discharge and organics, resulting in a decrease in plant diversity.

Zone 5, an intermediate marsh, is marked by minerogenic indicators (Mn/Rb, S/Rb), the organic indicator Br, and a rapid decrease in *Typha* abundance and pollen concentrations, implying reduced fluvial input and subsidence, resulting in low plant diversity.

Zone 6, the brackish marsh, is marked by strong correlations between Mn/Rb, saline, and brackish variables, indicating increasing salinity and water-logged conditions, driven by coastal retreat and RSLR. The terrestrial (Zr/Rb, Ti/Rb), minerogenic (Mn/Rb) and organic (Br) indicators are likely results of the marsh restoration projects.

Table 1 Summary table.

Zone/Age cal yr BP	Indicators	Depositional environment	Overall control	Active delta lobe
Zone 1 (3200)	Marine, biogenic, terrestrial	Fluvial deposition in an open bay	Initiation of delta progradation, geographical location	St. Bernard
Zone 2 (2300)	Terrestrial, hydrophytes, organic	Subaerial fluvial delivery of sediment and water	Delta progradation	St. Bernard
Zone 3 (1420)	Terrestrial, organic, various plant communities	Abandoned channels and newly created distributaries	Maximum delta development	St. Bernard & Lafourche
Zone 4 (920)	Freshwater aquatic herbs, insignificance of several terrestrial indicators	Reduced fluvial discharge	Decreased hydraulic efficiency during the delta transgressive phase	Lafourche
Zone 5 (330)	Minerogenic, organic, rapidly deceased Typha	Reduced fluvial input, subsidence	Delta abandonment	Lafourche &Plaquemines and Balize
Zone 6 (1972 CE)	Mn/Rb, saline, brackish	Marine transgression	Coastal retreat, RSLR	Plaquemines and Balize

The PCA biplots can be used to identify the different depositional processes dominating each ecosystem zone, which can then be used to infer the change in external forcing agent(s) driving each transition. In the early stage of coastal wetland evolution, the main driver of the ecological shifts was the delta cycle (progradation and abandonment). Following abandonment, ecosystem transitions were driven by more general coastal processes, including subsidence, RSLR, and, most recently anthropogenic activities.(see Table 1)

6. Conclusions

This study is an attempt to holistically reconstruct the environment from a site in Barataria Bay, southeast Louisiana, over the last 3200 years, describing not only the six successive ecosystems that occupied the site, but, in addition, evaluating the level of species diversity for each ecosystem, and, most importantly, identify both the depositional processes generating the physical conditions and the underlying forcing agent(s).

The six stages of ecosystem proceed from a subaqueous inter-distributary bay (3.2-2.3 cal kyr BP) with elevated terrestrial fluxes (Zr/Rb, Ti/Rb), to a hydrophyte freshwater marsh with aquatic vegetation (2.3-1.42 cal kyr BP) and elevated K/Ti and Mn/Rb ratios, to a mesophyte coastal prairie with elevated Br concentration, surrounded by diverse trees and flowering plants (1.42-0.92 cal kyr BP), to a *Typha* dominated freshwater marshland (0.92-0.33 cal kyr BP) with elevated Ti/Rb ratio, to an intermediate marsh, marked by an elevated minerogenic proxy and a rapid decrease in *Typha* abundance (0.33 cal kyr BP - 1972 CE), and, finally to a brackish marsh, with elevated levels of marine elements (Sr, Ca) and higher Mn/Rb ratios, and the occurrence of *Spartina* pollen.

The level of plant diversity is strongly correlated with the Mississippi delta cycle, with diversity increasing significantly during delta progradation, and decreasing significantly during transgression. The highest diversity occurs during the period of maximum delta-growth, correlating to the period of greatest geomorphic heterogeneity (e.g., oxbow lakes, levees, and point bars). The lowest diversity occurs during delta transgression, as subsidence reduces the geomorphic heterogeneity.

Multivariate PCA biplots are used to identify the primary depositional processes occurring during each zone, which are then used to infer the proximate, large-scale forcing agent(s). In the early stages, the main driver was the delta cycle, during both progradation and transgression. After the delta cycle ceased affecting the area the ecological shifts were driven by subsidence, marine transgression, and, most recently, anthropogenic activities.

These efforts to quantify ecosystem diversity and identify the physical processes driving shifts in the ambient background parameters are important, as understanding and identifying the physical mechanisms and external controls affecting the biological, chemical, and geological processes at any specific site, are necessary knowledge for evaluating/predicting the vegetative response to changing conditions.

The most important conceptual finding is that the relative importance of the various forcing agents and the relationships between them change over time; therefore, it is of crucial importance to understand exactly the background control(s) over the existent ecosystem at any specific time and location. This is of particular importance in terms of devising schemes for combatting important societal stresses, such as coastal erosion. The foremost implication from this study is that, due to the temporal and spatial variability of the processes driving the health and development of coastal ecosystems, a "one-size fits all" approach is not viable when dealing with important stresses in dynamic coastal environments. This is especially true in Louisiana due to the massive impact of the Mississippi River. The same argument can be applied to other large river deltas. The extreme economic importance of these deltas makes efforts to retard the deleterious effects of climate change, a societal necessity. Because the establishment and maintenance of healthy vegetative communities is a key step in protecting these deltas, understanding both the depositional processes controlling physical conditions, and identifying the underlying forcing agent is crucial. The datasets presented herein produce a methodology, likely globally applicable, for doing exactly that.

Author contributions

Junghyung Ryu Conceptualization-Lead, Data curation-Lead, Formal analysis-Lead, Investigation-Lead, Methodology-Equal, Project administration-Equal, Resources-Equal, Software-Lead, Visualization-Lead, Writing-original draft-Lead Kam-biu Liu Conceptualization-Equal, Formal analysis-Equal, Funding acquisition-Lead, Investigation-Equal, Methodology-Lead, Project administration-Lead, Resources-Lead, Supervision-Lead, Validation-Equal, Writing-review & editing-Lead Terry McCloskey, Writing-review & editing-Supporting.

Declaration of competing interest

The authors declare that they have no known competing financial interests or personal relationships that could have appeared to influence the work reported in this paper.

Data availability

Data will be made available on request.

Acknowledgments

This study was supported by grants from the National Science Foundation (NSF #1759715, 1212112). We thank Alejandro Antonio Aragón-Moreno for his help in the field.

Appendix A. Supplementary data

Supplementary data to this article can be found online at https://doi.org/10.1016/j.quascirev.2022.107865.

References

- Allison, M.A., Bianchi, T.S., McKee, B.A., Sampere, T.P., 2007. Carbon burial on riverdominated continental shelves: impact of historical changes in sediment loading adjacent to the Mississippi River. Geophys. Res. Lett. 34 (1).
- Authority, C. P. a. R., 2020. Annual Plan Fiscal Year 2020: Integrated Ecosystem Restoration and Hurricane Protection in Coastal Louisiana. Coastal Protection and Restoration Authority. Retrieved from.
- Banks, P., Beck, S., Chapiesky, K., Isaacs, J., 2016. Louisiana Oyster Fishery Management Plan. Louisiana Department of Wildlife and Fisheries, Office of Fisheries, Baton Rouge. LA.
- Berglund, B.E., Gaillard, M.-J., Björkman, L., Persson, T., 2008. Long-term changes in floristic diversity in southern Sweden: palynological richness, vegetation dynamics and land-use. Veg. Hist. Archaeobotany 17 (5), 573–583.
- Birks, H.J.B., Line, J., 1992. The use of rarefaction analysis for estimating palynological richness from Quaternary pollen-analytical data. Holocene 2 (1), 1–10.
- Blaauw, M., 2010. Methods and code for 'classical' age-modelling of radiocarbon sequences. Quat. Geochronol. 5 (5), 512–518.
- Blott, S.J., Pye, K., 2001. GRADISTAT: a grain size distribution and statistics package for the analysis of unconsolidated sediments. Earth Surf. Process. Landforms 26 (11), 1237–1248.
- Boesch, D.F., 1982. Proceedings Of the Conference On Coastal Erosion And Wetland Modification In Louisiana: Causes, Consequences, and Options: National Coastal Ecosystems Team. Office of Biological Services, Fish.
- Boonstra, M., Ramos, M., Lammertsma, E., Antoine, P., Hoorn, C., 2015. Marine connections of Amazonia: evidence from foraminifera and dinoflagellate cysts (early to middle Miocene, Colombia/Peru). Palaeogeogr. Palaeoclimatol. Palaeoecol. 417, 176–194.
- Buechakd, E.F., 1925. Bauxite in Northeastern Mississippi. Retrieved from The geology and agriculture of the State of Mississippi.
- Burton, E.D., Bush, R.T., Johnston, S.G., Sullivan, L.A., Keene, A.F., 2011. Sulfur biogeochemical cycling and novel Fe–S mineralization pathways in a tidally reflooded wetland. Geochem. Cosmochim. Acta 75 (12), 3434–3451. https://doi.org/10.1016/j.gca.2011.03.020.
- Chamberlain, E.L., Törnqvist, T.E., Shen, Z., Mauz, B., Wallinga, J., 2018. Anatomy of Mississippi Delta growth and its implications for coastal restoration. Sci. Adv. 4 (4), 4740.
- Chao, A., Gotelli, N.J., Hsieh, T., Sander, E.L., Ma, K., Colwell, R.K., Ellison, A.M., 2014. Rarefaction and extrapolation with Hill numbers: a framework for sampling and estimation in species diversity studies. Ecol. Monogr. 84 (1), 45–67.
- Chao, A., Kubota, Y., Zelený, D., Chiu, C.-H., Li, C.-F., Kusumoto, B., Yasuhara, M., Thorn, S., Wei, C.-L., Costello, M.J., Colwell, R.K., 2020. Quantifying sample completeness and comparing diversities among assemblages. Ecol. Res. 35 (2), 292–314. https://doi.org/10.1111/1440-1703.12102.
- Chao, Y., Mao, Y., Wang, Z., Zhang, T., 2015. Diversity and functions of bacterial community in drinking water biofilms revealed by high-throughput sequencing. Sci. Rep. 5 (1), 1–13.
- Chen, Y., Shen, L., Huang, T., Chu, Z., Xie, Z., 2020. Transformation of sulfur species in lake sediments at Ardley Island and Fildes Peninsula, king George Island, Antarctic Peninsula. Sci. Total Environ. 703, 135591. https://doi.org/10.1016/j.scitotenv.2019.135591.
- Chen, Z., Song, B., Wang, Z., Cai, Y., 2000. Late Quaternary evolution of the sub-aqueous Yangtze Delta, China: sedimentation, stratigraphy, palynology, and deformation. Mar. Geol. 162 (2), 423–441.
- Chmura, G.L., Smirnov, A., Campbell, I.D., 1999. Pollen transport through distributaries and depositional patterns in coastal waters. Palaeogeogr. Palaeoclimatol. Palaeoecol. 149 (1), 257–270.
- Cobb, R., Fred, T., Andrus, C., Etayo-Cadavid, M., 2009. Rangia Cuneata Shells as an Environmental Proxy: Variations in Elemental Concentrations within Populations, vol. 9.
- Conner, W., Day, J.W., 1987. The Ecology of Barataria Basin. Louisiana: an estuarine profile.
- Couvillion, B.R., Beck, H., Schoolmaster, D., Fischer, M., 2017. Land Area Change in Coastal Louisiana (1932 to 2016), 2329-132X. Retrieved from
- Cox, P.A., 1983. Search theory, random motion, and the convergent evolution of pollen and spore morphology in aquatic plants. Am. Nat. 121 (1), 9–31.
- Crowder, A.A., Cuddy, D., 1972. Pollen in a small River basin: Wilton Creek, Ontario. In: Birks, H.J.B., West, R.G. (Eds.), Symposium of the British Ecological Society. Blackwell, Oxford, pp. 61–77. Quaternary Plant Ecology.
- Culligan, N., Liu, K.-b., Ribble, K., Ryu, J., Dietz, M., 2022. Sedimentary records of

- microplastic pollution from coastal Louisiana and their environmental implications. J. Coast Conserv. 26 (1), 1–14.
- Currie, D.J., Mittelbach, G.G., Cornell, H.V., Field, R., Guégan, J.-F., Hawkins, B.A., Kaufman, D.M., Kerr, J.T., Oberdorff, T., O'Brien, E., Turner, J.R.G., 2004. Predictions and tests of climate-based hypotheses of broad-scale variation in taxonomic richness. Ecol. Lett. 7 (12), 1121–1134. https://doi.org/10.1111/j.1461-0248.2004.00671.x.
- Day, J.W., Lane, R.R., D'Elia, C.F., Wiegman, A.R.H., Rutherford, J.S., Shaffer, G.P., Brantley, C.G., Kemp, G.P., 2016. Large infrequently operated river diversions for Mississippi delta restoration. Estuar. Coast Shelf Sci. 183 (B), 292–303. https:// doi.org/10.1016/i.ecss.2016.05.001.
- Dean, J.W.E., 1974. Determination of carbonate and organic matter in calcareous sediments and sedimentary rocks by loss on ignition: comparison with other methods. J. Sediment, Res. 44 (1).
- Donahoe, R., Liu, C., Dobson, K., Graham, E., 1994. Cycling of iron and manganese in a Riparian wetland. Mineral. Mag. 58 (1), 237–238.
- Faegri, K., Kaland, P.E., Krzywinski, K., 1989. Textbook of Pollen Analysis. John Wiley & Sons Ltd.
- Frazier, D.E., 1967. Recent deltaic deposits of the Mississippi River: their development and chronology. Gulf Coast Assoc. Geol. Soc. Trans. 17, 287–315.
- Gonzalez, J.L., Törnqvist, T.E., 2009. A new Late Holocene sea-level record from the Mississippi Delta: evidence for a climate/sea level connection? Quat. Sci. Rev. 28 (17–18), 1737–1749.
- Gornitz, V., Lebedeff, S., Hansen, J., 1982. Global sea level trend in the past century. Science 215 (4540), 1611–1614.

 Hodell, D.A., Channell, J.E., Curtis, J.H., Romero, O.E., Röhl, U., 2008. Onset of
- Hodell, D.A., Channell, J.E., Curtis, J.H., Romero, O.E., Röhl, U., 2008. Onset of "Hudson strait" Heinrich events in the eastern north Atlantic at the end of the middle Pleistocene transition 640 ka)? Paleoceanography 23 (4).
- Hsieh, T., Ma, K., Chao, A., 2016. iNEXT: an R package for rarefaction and extrapolation of species diversity (H ill numbers). Methods Ecol. Evol. 7 (12), 1451–1456
- Jankowski, K.L., Törnqvist, T.E., Fernandes, A.M., 2017. Vulnerability of Louisiana's coastal wetlands to present-day rates of relative sea-level rise. Nat. Commun. 8, 14792.
- Juggins, S., 2007. C2: Software for Ecological and Palaeoecological Data Analysis and Visualisation (User Guide Version 1.5). Newcastle University, Newcastle upon Tyne. p. 77.
- Levin, D.R., 1990. Transgressions and Regressions in the Barataria Bight Region of Coastal Louisiana. LSU Historical Dissertations and Theses. Available from EBSCOhost geh database, 5072.
- Liu, K., Lu, H., Shen, C., 2008. A 1200-year proxy record of hurricanes and fires from the Gulf of Mexico coast: testing the hypothesis of hurricane—fire interactions. Quat. Res. 69 (1), 29–41.
- Löwemark, L., Chen, H.F., Yang, T.N., Kylander, M., Yu, E.F., Hsu, Y.W., Lee, T.Q., Song, S.R., Jarvis, S., 2011. Normalizing XRF-scanner data: a cautionary note on the interpretation of high-resolution records from organic-rich lakes. J. Asian Earth Sci. 40 (6), 1250–1256. https://doi.org/10.1016/j.jseaes.2010.06.002.
- Malacara, D., 2003. Color vision and colorimetry: theory and applications. Color Res. Appl. 28 (1), 77–78.
- Moore, H., 1899. Report on the Oyster-Beds of Louisiana. US Government Printing Office.
- Palazzesi, L., Barreda, V.D., Cuitiño, J.I., Guler, M.V., Tellería, M.C., Santos, R.V., 2014. Fossil pollen records indicate that Patagonian desertification was not solely a consequence of Andean uplift. Nat. Commun. 5, 3558.
- Pester, M., Knorr, K.-H., Friedrich, M., Wagner, M., Loy, A., 2012. Sulfate-reducing microorganisms in wetlands – fameless actors in carbon cycling and climate change. Front. Microbiol. 3. https://doi.org/10.3389/fmicb.2012.00072.
- Rodrigues, E., Cohen, M.C.L., Liu, K.-b., Pessenda, L.C.R., Yao, Q., Ryu, J., Rossetti, D., de Souza, A., Dietz, M., 2021. The effect of global warming on the establishment of mangroves in coastal Louisiana during the Holocene. Geomorphology 381, 107648. https://doi.org/10.1016/j.geomorph.2021.107648.
- Rothwell, R.G., Croudace, I.W., 2015. Twenty years of XRF core scanning marine sediments: what do geochemical proxies tell us?. In: Micro-XRF Studies of Sediment Cores. Springer, pp. 25–102.
- Ryu, J., Bianchette, T.A., Liu, K., Yao, Q., Maiti, K.D., 2018. Palynological and geochemical records of environmental changes in a Taxodium swamp near Lake Pontchartrain in southern Louisiana (USA) during the last 150 years. J. Coast Res. 85, 381–385. Special Issue.
- Ryu, J., Liu, K.-b., McCloskey, T.A., 2022a. The use of multivariate PCA dataset in identifying the underlying drivers of critical stressors, looking at global problems through a local lens. Data Brief. https://doi.org/10.1016/j.dib.2022.107946, 107946.
- Ryu, J., Liu, K., Bianchette, T.A., 2021a. Holocene environmental history of a freshwater wetland in southern Louisiana: a sedimentary record of delta development, coastal evolution and human activity. J. Quat. Sci. 36, 980–990. https://doi.org/10.1002/jqs.3324.
- Ryu, J., Liu, K., Bianchette, T.A., McCloskey, T., 2021b. Identifying forcing agents of environmental change and ecological response on the Mississippi River Delta, Southeastern Louisiana. Sci. Total Environ. 794, 148730. https://doi.org/10.1016/ j.scitotenv.2021.148730.
- Ryu, J., Liu, K., McCloskey, T.A., 2022b. Temporal variability in the relative strength of external drivers controlling ecosystem succession in a coastal wetland near Bayou Lafourche, southeast Louisiana, USA. Quat. Sci. Rev. 276, 107292. https:// doi.org/10.1016/j.quascirev.2021.107292.
- Saucier, R.T., 1968. Recent Geomorphic History Of the Pontchartrain Basin, Louisiana.

- (Doctoral Dissertation). Louisiana State University, LSU Historical Dissertations and Theses, 1418.
- Schmidt, C.W., 2015. Delta subsidence: an imminent threat to coastal populations. Environ, Health Perspect, 123 (8), A204-A209, https://doi.org/10.1289/ehp.123-
- Shaw, T.J., Moore, W.S., Kloepfer, J., Sochaski, M.A., 1998. The flux of barium to the coastal waters of the southeastern USA: the importance of submarine groundwater discharge. Geochem. Cosmochim. Acta 62 (18), 3047–3054.
- Shirazi, M.A., Hart, J.W., Boersma, L., 1988. A unifying quantitative analysis of soil texture: improvement of precision and extension of scale. Soil Sci. Soc. Am. J. 52 (1), 181-190.
- Sternberg, E., Tang, D., Ho, T.-Y., Jeandel, C., Morel, F.M., 2005. Barium uptake and adsorption in diatoms, Geochem, Cosmochim, Acta 69 (11), 2745–2752.
- Stockmarr, I., 1971. Tablets with spores used in absolute pollen analysis. Pollen Spores 13, 615-621.
- Syvitski, J.P., Kettner, A.J., Overeem, I., Hutton, E.W., Hannon, M.T., Brakenridge. G.R., Day, J., Vörösmarty, C., Saito, Y., Giosan, L., 2009. Sinking deltas due to human activities. Nat. Geosci. 2 (10), 681–686.
- Törnqvist, T.E., Rosenheim, B.E., Hu, P., Fernandez, A.B., 2015. Radiocarbon dating and calibration. In: Shennan, I., Long, A.J., Horton (Eds.), Handbook of Sea-Level Research, BP, pp. 349-360.
- Törnqvist, T.E., Wallace, D.J., Storms, J.E., Wallinga, J., Van Dam, R.L., Blaauw, M., Derksen, M.S., Klerks, C.J., Meijneken, C., Snijders, E.M., 2008. Mississippi Delta subsidence primarily caused by compaction of Holocene strata, Nat. Geosci, 1 (3), 173.
- Tornqvist, T.r.E., González, J.L., Newsom, L.A., Van der Borg, K., De Jong, A.F., Kurnik, C.W., 2004. Deciphering Holocene sea-level history on the US Gulf coast: a high-resolution record from the Mississippi delta. Geol. Soc. Am. Bull. 116 (7-8), 1026-1039,
- Van Geel, B., Buurman, J., Brinkkemper, O., Schelvis, J., Aptroot, A., Van Reenen, G.,

- Hakbijl, T., 2003. Environmental reconstruction of a Roman Period settlement site in Uitgeest (The Netherlands), with special reference to coprophilous fungi. J. Archaeol. Sci. 30 (7), 873-883.
- Van Geel, B., Coope, G.R., Van Der Hammen, T., 1989. Palaeoecology and stratigraphy of the Lateglacial type section at Usselo (The Netherlands). Rev. Palaeobot. Palynol. 60 (1-2), 25-129.
- Visser, J.M., Duke-Sylvester, S.M., Carter, J., Broussard III, W.P., 2013. A computer model to forecast wetland vegetation changes resulting from restoration and protection in coastal Louisiana. J. Coast Res. 67 (sp1), 51-59.
- Wang, M., Wang, L., Zhao, S., Li, S., Lei, X., Qin, L., Sun, X., Chen, S., 2021. Manganese facilitates cadmium stabilization through physicochemical dynamics and amino acid accumulation in rice rhizosphere under flood-associated low pe+pH. J. Hazard Mater. 416, 126079. https://doi.org/10.1016/j.jhazmat.2021.126079.
- Wang, M., Zheng, H., Xie, X., Fan, D., Yang, S., Zhao, O., Wang, K., 2011, A 600-year flood history in the Yangtze River drainage: comparison between a subaqueous delta and historical records, Chin. Sci. Bull. 56 (2), 188–195.
- Weng, C., Hooghiemstra, H., Duivenvoorden, J.F., 2006. Challenges in estimating past plant diversity from fossil pollen data: statistical assessment, problems, and possible solutions. Divers. Distrib. 12 (3), 310–318.
 Willard, D.A., Bernhardt, C.E., Weimer, L., Cooper, S.R., Gamez, D., Jensen, J., 2004.
- Atlas of pollen and spores of the Florida Everglades. Palynology 28 (1), 175–227.
- Wilson, C.A., Allison, M.A., 2008. An equilibrium profile model for retreating marsh shorelines in southeast Louisiana. Estuar. Coast Shelf Sci. 80 (4), 483–494.
- Wodehouse, R.P., 1937. Pollen grains: their structure, identification and significance in science and medicine. J. Nerv. Ment. Dis. 86 (1), 104. Xu, K., Bentley, S.J., Day, J.W., Freeman, A.M., 2019. A review of sediment diversion in
- the Mississippi River Deltaic Plain. Estuar. Coast Shelf Sci. 225, 106241.
- Yakubik, J.K., Maygarden, B., Kidder, T.R., Dawdy, S., Jones, K., 1996. Archeological Data Recovery of the Camino Site (16JE223), A Spanish Colonial Period Site Near New Orleans, Louisiana. Retrieved from.